Bull. Min. Res. Exp. (2019) 158: 195-216

Bulletin of the Mineral Research and Exploration

http://bulletin.mta.gov.tr

Evaluation of soil geochemistry data of Canca Area (Gümüşhane, Turkey) by means of Inverse Distance Weighting (IDW) and Kriging methods-preliminary findings

Alaaddin VURAL[a*]

[a] *Gümüşhane University, Faculty of Engineering and Natural Sciences, Department of Geological Engineering, 29000, Gümüşhane, Turkey*
orcid.org/0000-0002-0446-828X

Research Article

Keywords:
Soil geochemistry, inverse distance weighting (IDW), kriging, Gümüşhane.

Received Date: 29.12.2017
Accepted Date: 29.05.2018

ABSTRACT

The purpose of this study is to assess soil geochemical data of the Canca alteration area (Gümüşhane-Turkey) using statistical methods and investigate potential gold mineralizations of the area. With this purpose, 288 soil samples were collected and analyzed for gold and associated pathfinder elements. The concentrations ranged (Au and Hg: in µg/kg, others in mg/kg) between 0,68-19,20; 0,02-28,97; 2-314; 7-857; 2,1-394; 4-199,5; 0,59-49,29; 5-89; 0,04-37; 0,52-16,30; 1,25-91,9 for Au, Ag, Cu, Pb, Zn, As, Sb, Bi, Mo, Sn and Hg respectively. According to Sperman's rho correlation coefficients, although not very strong, correlation was observed between Cu and Au; Zn and Cu; Sb and Pb and As; Mo and Pb and As and Sb; Sn and As; Sb and Mo. The threshold values of the elements were obtained by median+2 the median absolute deviation. The prediction maps of the elements were formed by using the Inverse Distance Weighting and Kriging methods. According to prediction maps; especially in the western part of the study area and also related to tectonic lines, elemental enrichments, (gold and silver) were determined. Therefore, it is suggested to give importance to the west of the area in exploration drilling, geophysics, etc. Since the element prediction maps produced by the Inverse Distance Weighting method has higher resolution in anomaly contrast, it is suggested that maps produced with this method can preferably be used to give an idea at first sight in soil geochemistry studies.

1. Introduction

Canca (Gümüşhane, NE Turkey) hydrothermal alteration area is approximately 10 km northwest of the Gümüşhane city center in the Black Sea Tectonic Unit in the Eastern Black Sea Region. There are many mineral deposits in various types such as porphyry, skarn and epithermal in the area where the study area is located (Koza gold mine, Gümüştaş zinc-lead copper mine, Yıldızlar zinc-lead copper mine, Arzular gold mine, Ünlüpınar lead mine, Kösdere copper-lead-zinc mine, Karadağ skarn, porphyry and vein type ores, Istala skarn type zinc-copper mine and etc.). There are many investigations carried out in Gümüşhane and its close vicinity mainly by the General Directorate of Mineral Research and Exploration (MTA), public and private organizations beginning from the second half of the 20th century because of its geological richness and host many mineral deposits. Many studies are in general geology, but most of them are in mineral exploration. Especially after the 1980s, such studies continued with acceleration.

Prospection studies on mineral exploration covering generally the whole Turkey and especially in the region were carried out mainly in the form of rock geochemistry and mining geology. As the rock geochemistry studies is directly related with mineralization they possess a significant place in exploration geochemistry studies and have a bigger role in detailed geochemistry studies.

General prospecting studies, one of the most important shortcomings of our country, are in fact

* *Corresponding author: Alaaddin VURAL, alaaddinvural@hotmail.com*
https://dx.doi.org/10.19111/bulletinofmre.430531

the most important and initial stages of detailed geochemical studies such as rock geochemical studies. Almost all developed countries in the world have completed their general prospection studies and have made great progress in detailed geochemical studies. Therefore, especially in recent years, the general prospection studies (soil, plant, water geochemistry) have been initiated by MTA.

As mentioned above, the rock geochemistry studies are more suitable for detailed prospection studies, however they are time consuming and do not always give any desired results when used in general prospections and/or in detailed studies alone. They also cause mineralizations to be missed in occasion in precious mineral deposits especially such as epithermal gold deposits. Especially in searching such mineral deposits; there are many encouraging mineral exploration stories and good results belonging to soil geochemistry and biogeochemistry studies which are carried out with the next stage of general prospection and even with the rock geochemistry.

The purpose of this study is to investigate the possible gold mineralization buried in the Canca (Gümüşhane-Turkey) hydrothermal alteration site, which was discovered during the prospection studies by MTA, using soil geochemistry by statistical methods. There, the mineral geochemistry studies were also performed from time to time as it was considered to be important in mineralization.

Works in the field seem to extend until 1980s when report records are taken into consideration. The preliminary studies are general mineral prospection studies carried out by Çınar et al. (1982) in the region. In this study, hydrothermal alterations in the area were pointed out. Güner et al. (1985) have mapped the hydrothermal alteration areas of the Canca area during the 1/5000 scale mapping studies of the Hazine Cave and Kırkpavli mineralizations located near the Canca site.

During the detailed study of the entire region within scope of the Turkish-Japanese Joint Project (MTA, 1986) co-operated with the Japan Cooperation Agency (JICA) in the 1980s the studies were carried out in order to determine the alterations in the Canca area, and attention was paid to hydrothermal alterations and scattered pyrite mineralizations.

Kansız et al. (1994) carried out prospection and geological investigations on a wide area in 1/5000 scale, including the study area, in 1989, 1990 and 1991. Within the scope of these studies, they carried out 1/10 000 scale geology and alteration mapping studies in the Canca area and detected values of 85-167 mg/kg Cu, 146 mg/kg Pb, 165 mg/kg Zn, 5-24 mg/kg Sb, 80-200 mg/kg As, 1.2-2 mg/kg Ag and 1 mg/kg Au in rock samples. In rock geochemical studies conducted by Güner and Yazıcı (2008), high Ag values of 1.2-5.1 mg/kg were reported. In another study conducted by the same researchers the values of 761 mg/kg As, 80 ppb Au and 2.7 mg/kg Ag (Yazıcı et al., 2014) were reported. In the context of the remarkable pathfinder element and other metals obtained, the silver and gold values are the data obtained from rock geochemistry studies.

No studies on soil and/or plant geochemistry have been found on the Canca alteration area. Despite the fact that mineral exploration studies were carried out in the area, the lack of soil geochemistry studies were noticed. Therefore; the soil geochemistry study was also carried out. There are many studies in the literature that use soil geochemistry in gold explorations. For example; Reis et al. (2001) showed that soil geochemistry studies had been effectively used in the exploration of gold mineralization in their studies. They also detailed the study area increasing the anomaly contrast resolution of the element distribution maps, which were formed by the soil geochemistry, using the method they suggested in the calculation of threshold value also benefiting especially from pathfinder elements.

In Çanakkale-Ayvacık and its close vicinity, the gold exploration was carried out by using soil geochemistry studies and the Kısacık gold field with a capacity of 10 tons of gold were found (Vural, 2006) by means of appropriate well sites given with soil geochemical studies. The soil geochemistry as well as plant geochemical studies has been an important method used in mineral explorations since 1950s. Satisfactory results have also been obtained with plant geochemical studies.

The soil geochemistry study in gold enrichments in the Arzular town (Gümüşhane province) located in the close vicinity of the study area was carried out by Yaylalı-Abanuz et al. (2012). Suggestions for suitable drilling locations for the area were also made with the study in which the element distribution maps were formed especially using the Kriging method. Soil geochemistry studies on the Kırkpavli alteration site were carried out by Vural and Erdoğan (2014), which is located at 1.5-2 km SSW of the Canca area. In this study; they asserted that elements of Ba, Zn, Pb, Ni, Mn, Cu, Cr and As could be used as pathfinder elements for gold, formed the anomaly maps of these elements for the area by the Kriging interpolation method and suggested suitable drilling locations for gold exploration. At the moment, a private company has completed drillings for gold exploration and initiated operational processes.

The purpose of this study is to investigate possible gold mineralization buried in the Canca (Gümüşhane) hydrothermal alteration site, which was discovered during the prospection studies by MTA, using soil geochemistry study by statistical methods. There, the mineral geochemistry studies were also performed from time to time as it was considered to be important in the mineralization.

In this context, the total of 288 soil samples collected for soil geochemistry from the Canca area were analyzed in the Central Laboratory of the Gümüşhane University and various statistical analyzes of the obtained data were performed. The threshold values of the elements were calculated benefiting from the Median Absolute Deviation (MAD) values of which their excessive values are attenuated and the potential of buried gold mineralization of the area was investigated by means of the produced element distribution maps.

2. General Geology of the Area

The study area is located at 10 km north-west of the Gümüşhane province and covers an area of approximately 1.5-2 km^2 (Figures 1 and 2). The geology of Gümüşhane and its surroundings, including the study area, is like a small summary of the geology of a significant part of the Eastern Black Sea Region. The investigation of the geological elements by these researchers here significantly contributes to the understanding of the Eastern Black Sea Tectonic Union (Ketin, 1966), which is known as the Eastern Pontides.

The basement of the Eastern Black Sea Tectonic Union in Gümüşhane and its surroundings is formed by the Kurtoğlu Metamorphics and the cutting unmetamorphosed granitic plutons (Gümüşhane Granitoid) (Dokuz, 2011; Topuz et al., 2007; Yılmaz, 1972). These metamorphic basement rocks outcrop in southwest of Gümüşhane outside the study area. The Gümüşhane Granitoid outcrops in many places, mainly in the Gümüşhane city center and is overlain by the Early-Middle Jurassic volcanoclastic unit (Şenköy formation) (Kandemir, 2004). The volcanoclastic unit grades into the carbonate rocks of the Late Jurassic and the Early Cretaceous formations of Pelin (1977) called the Bergida formation in the upper layers. The carbonate rocks are then conformably overlain by the Late Cretaceous clastic units (Kermutdere formation) (Tokel, 1972) (Figure 1).

The Kermutdere formation, which begins with the deposition of sandy limestone at the bottom, grades into red pelagic limestones and a turbiditic series consisting of sandstone, siltstone, marl and limestones in the upper layers. All these units are then cut by the Late Cretaceous intrusions in the northwestern part of the study area (Kaygusuz et al., 2008). Late Cretaceous plutonic, volcanic and sedimentary rocks are stratigraphically overlain by the Middle-Late Eocene volcanic and volcanoclastic rocks (Arslan and Aliyazıcıoğlu, 2001; Güven, 1993). These units are called as the Alibaba formation in the region (Tokel, 1972). Alibaba formation is cut by the synchronous calc-alkaline granitoids (Eyüboğlu et al., 2011; Karslı et al., 2013) called the Gözeler granite (Vural, 2017, 2014) which outcrops in close vicinity of the study area.

2.1. Stratigraphy of the Study Area and Alteration Development Process

The Middle-Late Eocene Alibaba formation outcrops in the study area. The unit is formed by basalt and andesite in the study area and is occasionally cut by andesite-dolerite dykes which are the final product of the Eocene volcanism. In close vicinity of the study area the Gözeler granite, which is considered to be Upper Eocene (?) is observed in south of the area (Figure 1). It is predicted that the alteration in the area and possibly buried mineralization might have developed due to the Upper Eocene granitic intrusive rocks which outcrop in many areas such as Gözeler (Old Gümüşhane), Avliya (Torul-Gümüşhane), Demirören-Sarıçiçek-Dölek (Gümüşhane-Center) in the region and the Upper Cretaceous granitic rocks in northwest of the study area. Hydrothermal fluids, mainly the products of the Upper Eocene processes, have reached shallow geochemical environments along the tectonic lines developed as a result of the neotectonic evolution of the region and altered the predominantly andesitic rocks in the Canca area.

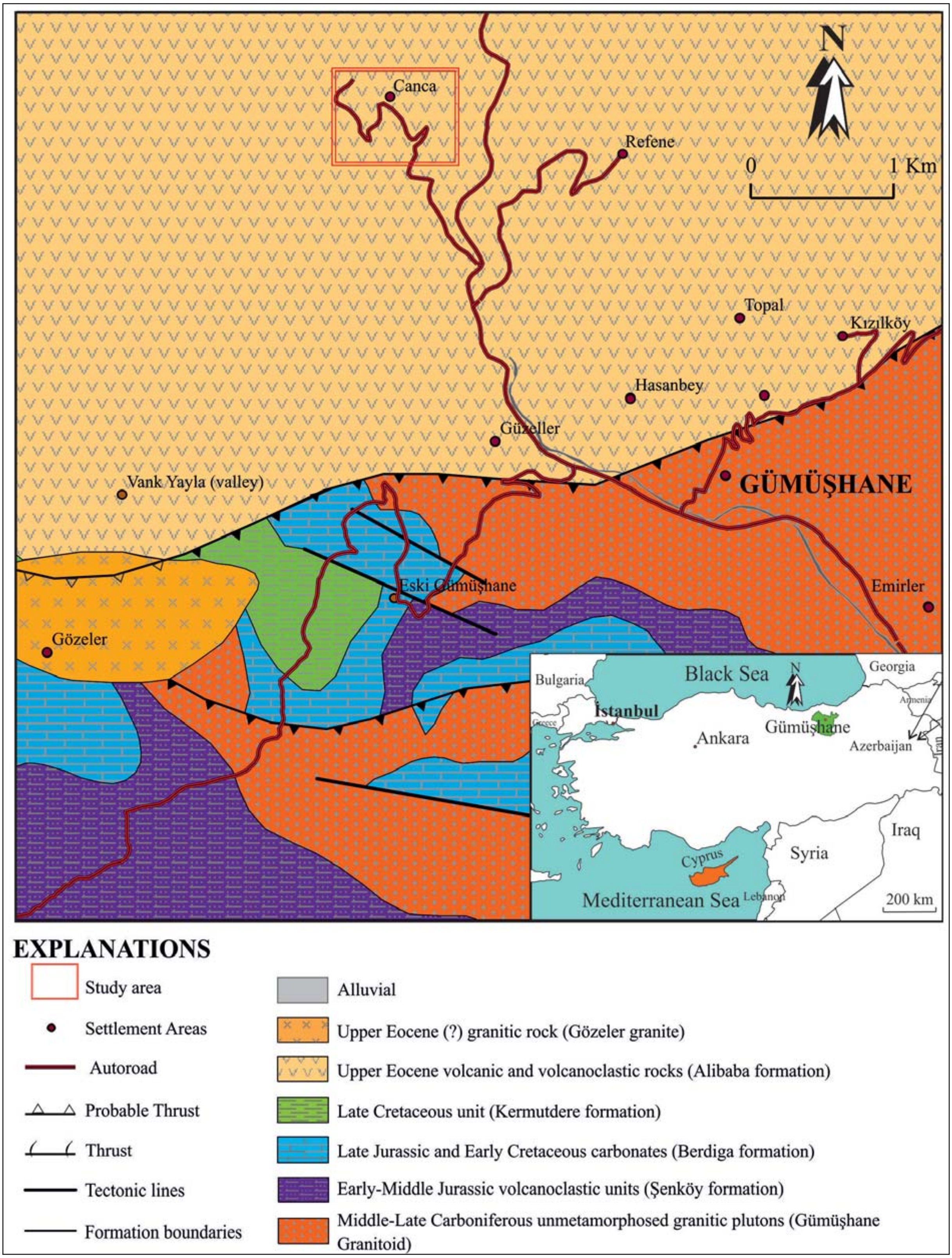

Figure 1- Geological map of Gümüşhane and its close vicinity (modified from Güven, 1993).

Therefore, the alteration-mineralization in the field is tectonical and caused the alteration of the final product fluids of buried granitoidic rocks in the area in surrounding rocks. The fluids along tectonic lines, which are dominantly in E-W, slightly NW-SE directions in accordance with the development of the neotectonic roof of the region, have altered the field along these lines (Figure 2).

Silicifications (phyllic alteration) important for the mineralization have developed along tectonic lines in E-W and NW-SE directions. In particular, the intense hydrothermal alteration (silicification, argillization, hematitization, limonitization and pyritization) is observed along fracture lines. The silicification covers a wider area especially in the western part of the landscape. Kaolinite, smectite and illite have gained importance in the remaining altered section where alunite, chalcedony, gypsum vein and veinlets are seen.

2. Material and Method

In context of soil geochemistry studies, the total of 288 soil samples were collected along NE/SW and NW/SE profiles in the Canca alteration site (Figure 2). Samples were collected, numbered and placed into nylon bags using plastic shovels from a depth of 0-25 cm (zone B of the soil profile) in such a way as not to cause any geochemical contamination and in accordance with the sampling standards for clean nylon bags. Soil specimens were prepared by routine analyze preparing works in the Geological Engineering Laboratory of the Faculty of Engineering and Natural Sciences at the Gümüşhane University. In this context, it was ensured that the samples were dried under natural conditions in a non-humidity environment, then the product was dried at 60°C for 2 days and the natural moisture was removed. Then, the samples were sieved under 2 mm polyethylene sieve and the samples passing through the sieve were milled with a ring mill. They then passed through 80-mesh sieve to obtain 10-15 g packages from soil samples in ideal sizes suggested by Rose et al. (1991). The soil pH measurements were also made at the Geochemistry Laboratory in the Geological Engineering Department at the Gümüşhane University. Soil samples for soil pH measurements were sieved under 100 mesh size and the samples, of which their natural humidities were removed by leaving them in an oven for 2 days under 60°C, were mixed by sample/distilled water mixture in 2/2,5 mass(gr)/volume(mL) ratio then placed into 50 mL flacon tubes. Samples were then rinsed 60 minutes on the shaking table and left 10 hours for suspended materials to settle down. Finally, their pH measurements were made using the Hanna brand desktop pH meter. It was determined that the pH of the soil changed between 3.90 and 7.02 and therefore it was detected that the acidity of the Canca field was higher.

The soil samples were analyzed by ICP-MS (Inductively Coupled Plasma–Mass Spectrometer) in the Central Laboratory of the Gümüşhane University

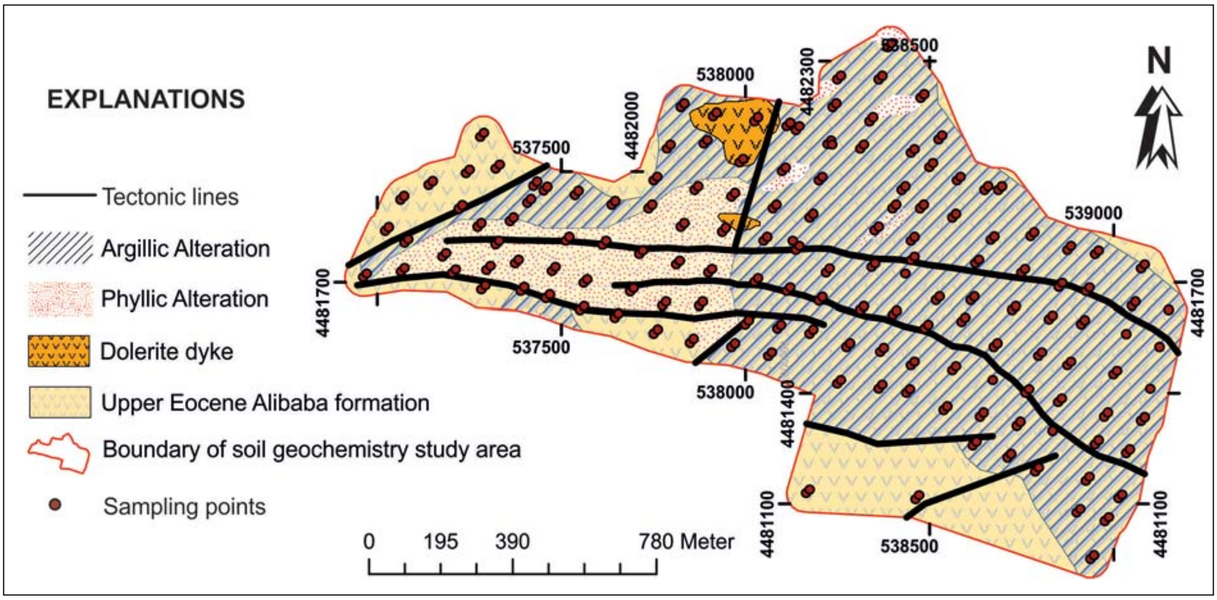

Figure 2- Geology and alteration map of the study area (modified from Güner and Yazıcı, 2008).

after dissolution in the closed circuit microwave dissolution system. From soil samples powdered during analysis, the measurements around 0,20 g (in 0,1 mg sensitivity) were taken and placed in the Teflon beaker of the microwave oven (AGILENT MDS-8G). By adding 4 mL of NHO_3 and 2 mL of HF, they were subjected to the fragmentation under conditions given in table 1 (1st stage), then they again were subjected to the fragmentation under conditions given in table 1 (2nd stage) by adding this time 5 mL of B_3OH_3 to the resulting solution. After the treatment, clear solutions obtained by which the beaker contents were obtained after filtering through glass wool, were quantitatively completed to 50 mL by adding distilled water and analyzed. In order to control the reliability of results; each sample was re-analyzed at least 3 times, the mean and standard deviations of the results were calculated to determine the accuracy and the results were given at a certain reliability interval and level. In addition to using the standard calibration graph, the standard addition to samples and internal standard methods were applied. Besides, the accuracy tests have also been completed by applying the Standard Reference Material (SRM) to the sample solutions by applying spiked/recovery tests. The performance and accuracy of the method applied are; as the soil SRM; sandy soil standard "Sandy Soil C (CRM-SA C)" were used and the quality control/quality assurance (QC/QA) parameters obtained were given in table 2.

3. Results and Discussion

The major and trace element analyzes of soil samples collected from the Canca area were carried out in the Central Laboratory of the Gümüşhane University using ICP-MS instrument and the descriptive statistical parameters of the gold and geochemically related elements were given in table 3. When the results obtained are evaluated, it is seen that the elements exceed the upper crustal values suggested by Rudnick and Gao (2010) at some sampling points. Therefore, there is an enrichment by the elements in the area.

Elements were subjected to Kolmogorov-Smirnov and Shapiro-Wilk normality tests and checked for their normal distribution. Since the significance level was found to be less than 5% for both tests it was seen that data of which their Ho hypothesis (the data showing

Table 1- Partition program in microwave oven.

1st Stage				2nd Stage			
Level	Temperature (°C)	Time (min.)	Power (Watt)	Level	Temperature (°C)	Time (min.)	Power (Watt)
1	120	5	800	1	120	6	800
2	130	5	800	2	130	6	800
3	150	5	800	3	150	6	800
4	210	7	800	4	210	10	800

Table 2- Accuracy tests of analyses.

	Na	Mg	Al	S	K	Ca	V	Cr	Mn	Fe	Co	Ni	Cu
Lower limit, LOD, µg/L	2,3	1,0	1,4	3,4	3,4	3,8	0,12	0,05	0,11	2,0	0,02	0,17	0,09
Lower limit, LOD, µg/kg	575	250	350	850	850	950	30	12,5	27,5	500	5	42,5	22,5
Upper limit, mg/L	100	100	100	100	100	100	10	10	10	100	10	10	10
Upper limit, mg/kg	25000	25000	25000	25000	25000	25000	2500	2500	2500	25000	2500	2500	2500
RSD, %	1,2	3,4	4,9	4,8	2,2	3,1	2,5	1,7	1,1	2,6	2,5	1,9	0,7
	Zn	**As**	**Se**	**Sr**	**Mo**	**Ag**	**Cd**	**Sn**	**Sb**	**Ba**	**Au**	**Hg**	**Pb**
Lower limit, LOD, µg/L	0,52	0,07	0,06	0,12	0,05	0,01	0,02	0,12	0,25	0,00015	0,01	0,01	0,12
Lower limit, LOD, µg/kg	130	17,5	15	30	12,5	2,5	5	30	62,5	0,0375	2,5	2,5	30
Upper limit, mg/L	10	10	10	10	10	10	10	10	10	10	10	10	10
Upper limit, mg/kg	2500	2500	2500	2500	2500	2500	2500	2500	2500	2500	2500	2500	2500
RSD, %	3,3	1,9	2,2	1,6	2,1	1,5	0,6	3,3	2,9	1,9	0,6	1,1	2,1

LOD, Limit of Detection,
RSD, Relative Standard Deviation,

Table 3- Descriptive statistical values of the elements and calculated threshold values with respect to different statistical parameters.

	Au µg/kg	Ag mg/kg	Cu mg/kg	Pb mg/kg	Zn mg/kg	As mg/kg	Sb mg/kg	Bi mg/kg	Mo mg/kg	Sn mg/kg	Hg µg/kg
Amount	39	89	285	269	285	287	142	40	75	124	69
Minimum	0,68	0,02	2,00	7,00	2,10	4,00	0,59	5,00	0,04	0,52	1,25
Maximum	19,20	28,95	314,00	857,57	394,00	199,95	49,29	89,00	37,00	16,30	91,90
Mean	6,97	2,44	69,42	80,61	74,45	37,98	8,00	18,28	5,30	1,53	23,65
Geo. Mean.	5,36	0,69	55,01	55,84	63,29	28,92	4,55	13,36	2,35	1,31	19,60
Median	5,40	0,54	68,00	52,72	70,00	29,06	4,27	12,00	2,63	1,25	21,20
SD	4,83	4,75	42,93	103,76	39,96	31,10	9,65	17,72	7,53	1,52	15,08
Skewness	0,88	3,40	1,61	4,64	2,40	2,20	2,40	2,39	2,62	7,78	2,43
Kurtosity	-0,11	13,20	6,71	26,86	15,10	6,23	6,25	6,43	6,73	73,66	8,55
Mean+2SD	16,62	11,93	155,29	288,14	154,36	100,19	27,30	53,72	20,36	4,57	53,81
Geo.M+2SD	15,01	10,18	140,88	263,37	143,20	91,13	23,85	48,81	17,41	4,34	49,76
Median+2MAD	11,60	1,42	120,00	98,16	91,00	57,34	10,20	24,00	6,77	1,50	32,00
Background values*	1,5	0,053	28	17	67	4,8	0,4	0,16	1,1	2,1	50

Geo.M.: Geometric Mean, SD: Standard deviation, MAD: Median Absolute Deviation
*from Rudnick and Gao (2010).

the normal distribution of the data) had been rejected was found to be non-normal distribution (Table 4). Histograms were created for visual evaluation of dataset distributions (Figure 3). When histograms and descriptive statistical parameters of the elements are considered, it is seen that the element sample groups are skewed rightward. Logarithmic values of the data for all elements were taken and histograms were regenerated (Figure 3). When histograms generated from logarithmic data were examined, it was seen that the distorted data did not form an ideal Gaussian population, although they were converted to some normal distribution. Performing Box-Cox and Arcsin transformations it was tested whether the distribution approached the Gaussian distribution or not. However, it was seen that the most ideal transformation was sub-sampling assemblage obtained only from logarithmic transformations.

Since elements did not show a normal distribution, the correlation of the elements with each other was examined by calculating the Spearman's rho correlation coefficients (Table 5). Spearman's rho correlation coefficients are between -1 and +1. If the correlation coefficient is +1, it can be said that there is an excellent positive linear relationship between the variables, if it is -1 then there is an excellent negative linear relationship between the variables. If the coefficient is 0 then it is understood that there is no linear relationship between the variables. Also according to the correlation coefficient intervals there is a classification as; very weak (0,00-0,25), weak (0,26-0,49), moderate (0,50-0,69), high (0,70-0,89), very high (0, 90-100), and the direction of relationship is stated according to the negative or positive value of the coefficients. Although it is not so strong according to the Spearman's rho correlation coefficients, the

Table 4- Normality tests for elements.

	Kolmogorov-Smirnov[a]			Shapiro-Wilk		
	Statistics	df	Sig.	Statistics	df	Sig.
Au (µg/kg)	0,183	39	0,002	0,908	39	0,004
Ag (mg/kg)	0,305	89	0,000	0,532	89	0,000
Cu (mg/kg)	0,062	285	0,009	0,900	285	0,000
Pb (mg/kg)	0,252	269	0,000	0,518	269	0,000
Zn (mg/kg)	0,094	285	0,000	0,859	285	0,000
As (mg/kg)	0,145	287	0,000	0,791	287	0,000
Sb (mg/kg)	0,221	142	0,000	0,704	142	0,000
Bi (mg/kg)	0,245	40	0,000	0,711	40	0,000
Mo (mg/kg)	0,263	75	0,000	0,637	75	0,000
Sn (mg/kg)	0,265	124	0,000	0,385	124	0,000
Hg (µg/kg)	0,184	69	0,000	0,781	69	0,000

a. Lilliefors (Sig.) correction, df:degree of freedom

Table 5- Spearson’s rho correlation coefficients among elements.

Spearman's rho	Au	Ag	Cu	Pb	Zn	As	Sb	Bi	Mo	Sn	Hg
Au	1,00										
Ag	0,14	1,00									
Cu	0,52**	0,31**	1,00								
Pb	-0,16	0,10	-0,21**	1,00							
Zn	0,26	0,38**	0,55**	-0,24**	1,00						
As	-0,31	0,25*	0,11	0,43**	-0,04	1,00					
Sb	-0,36*	0,06	0,08	0,47**	-0,03	0,74**	1,00				
Bi			-0,10	0,31	-0,25	0,23	0,42	1,00			
Mo	-0,07	0,41**	0,02	0,47**	-0,11	0,65**	0,51**	0,43	1,00		
Sn	-0,17	0,33**	0,01	0,37**	0,23*	0,58**	0,56**		0,46**	1,00	
Hg	-0,18	0,11	-0,16	0,11	-0,01	0,11	0,34**		0,05	0,19	1,00

*. Correlation weightiness value around 0,05 and two-tailed.
**. Correlation weightiness value around 0,01 and two-tailed.

presence of a correlation between Cu-Au; Zn-Cu; Sb-Pb-As; and between Mo-Pb, As-Sb; Sn-As, Sb-Mo were determined.

One of the most common problems for geochemical data is that although many methods have been tried for transformations, the ideal distribution cannot always be reached. In these cases, one of the methods especially used in the threshold calculation to reduce the effect of extreme end values is to determine the MAD value and calculate the threshold value (TV) (median +2MAD, (M +2MAD)) similar to the TV calculation preferred in classical methods (average +2standard deviations, geometric mean +2standard deviations and etc.). The reason why median (M) and MAD are used in TV calculation is that it shows less affection against excessive values and deviations (Tum et al., 2011). There are also other methods in TV calculation. Among them, the multifractal modellings are most common (Almasi et al., 2015, Anderson, 2008, Carranza, 2009, Carranza et al., 2009, Carranza and Sadeghi, 2010, Jena, 1996, Zuo et al., 2009). A more detailed evaluation of the field using the aforementioned methods and comparing the methods applied with each other will be carried out in another study.

The M+MAD method is a very useful and practical method for evaluating the initial findings and giving an idea about the site. The MAD method has been rediscovered by Hampel (1974), inspired by the ideas of Carl Friedrich Gauss (1777-1855), and widely recognized in the scientific literature. The MAD is calculated as follows:

$$MMS = M_i(|x_i - m_j(x_j)|) \qquad 1$$

where; xi is the number of each element in the sample, xj corresponds to the number of original observations, and Mi is the median of series.

The element distribution/anomaly maps generated by using threshold values obtained from M and MAD data give more realistic and satisfactory results (Reiman and Filzmoser, 2000).

Threshold values obtained by classical methods and by the M +2MAD method in this study are given in Table 3 for comparison. The calculated TVs are as follows: (M +2SD)> (Geo.M +2SD)> (M +2MAD).

3.1. Generation of Element Distribution Maps

Element distribution maps are the most common and ultimately used data evaluation stage in assessing the data in soil geochemistry studies for mineral exploration. The basic models used to generate the element distribution maps can be grouped under two main headings: Deterministic models and Probabilistic (linear statistic) models. The Inverse Distance Weighting (IDW) interpolation and Kriging methods are the best known methods for deterministic and probabilistic methods, respectively.

The IDW interpolation model is the oldest spatial prediction method (Shepard, 1968) and the easiest deterministic interpolation method. There are several decision-making methods to implement the model parameters and provide quick and easy information on the interpolated surfaces. It is preferred because it is easy and fast to use. To estimate the value at any unmeasured point, the IDW uses the measured values near the desired point to be estimated.

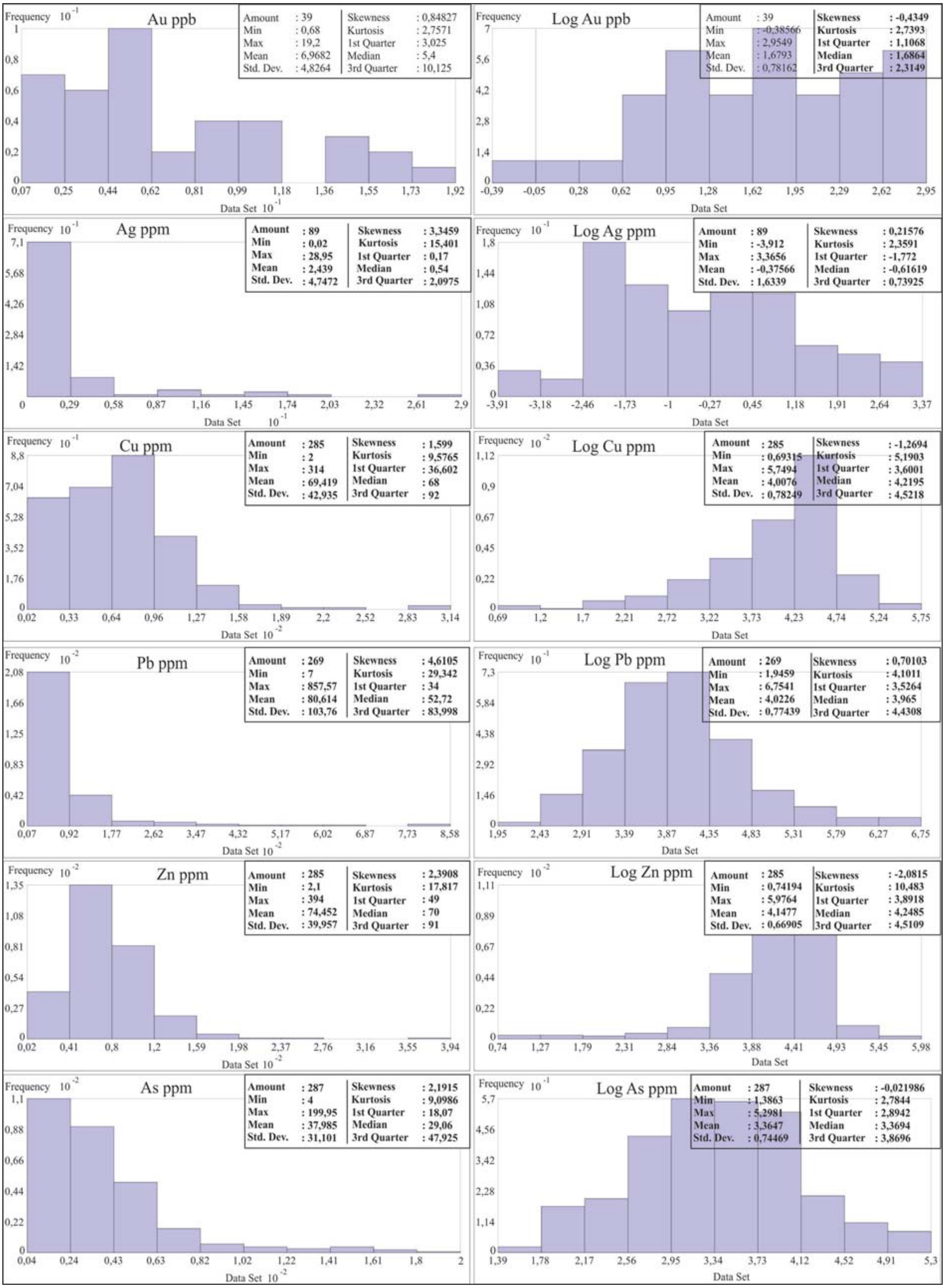

Figure 3- Histograms of raw and logarithmically transformed data.

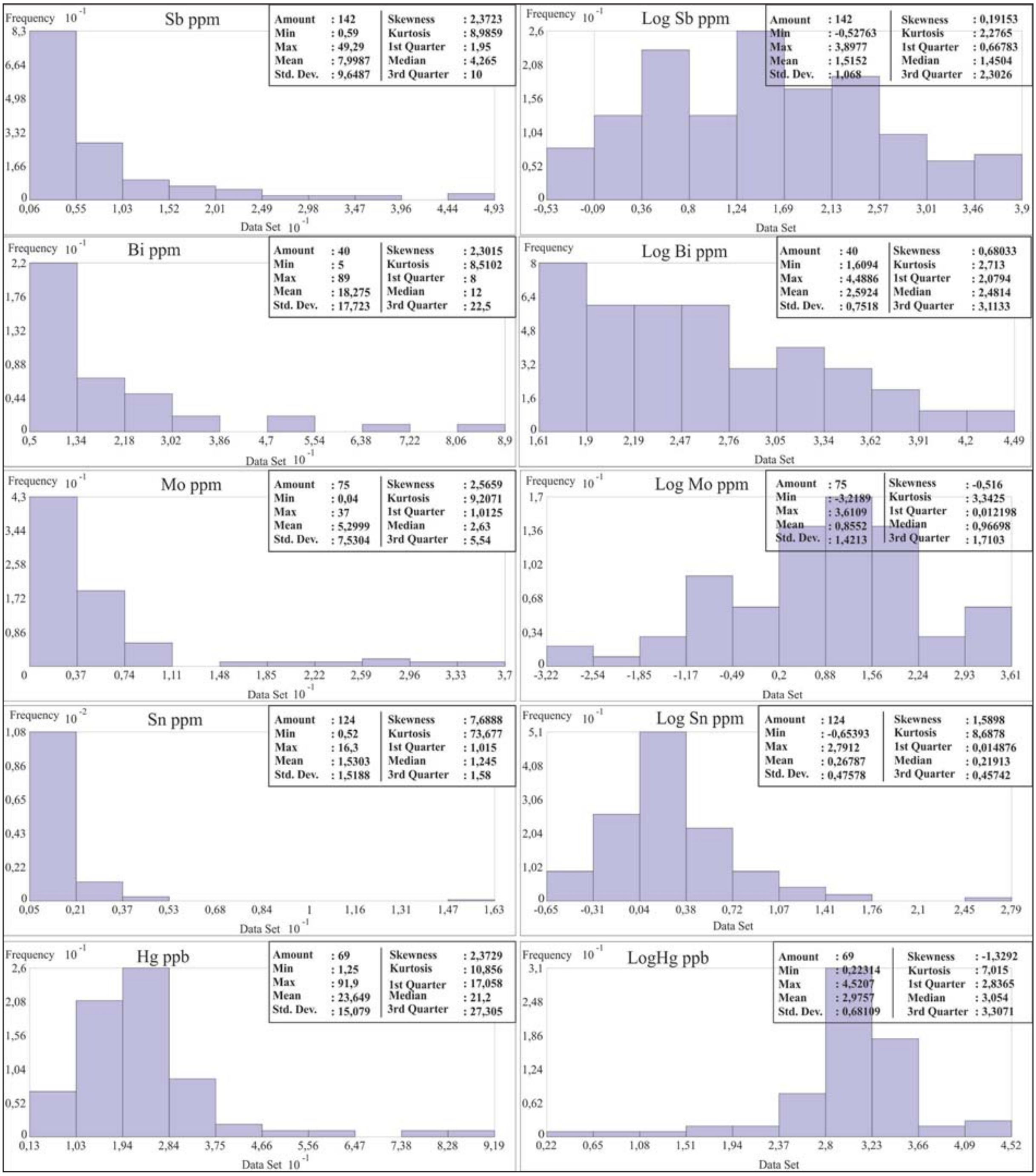

Figure 3- Continue.

The effect of the measured values closest to the desired point is more influential than the distances farthest to the investigated point. The fundamental of IDW was inspired by the principle of Waldo Tobler (Tobler, 1970) "*Everything is related to everything else, but the near ones are more related than the far ones*", the first law of Waldo Tobler in geography. Therefore, large weights are obtained from the points close to each other and small weights are obtained from distant points. Although there are several IDW methods, "Shaperd's Method" is the best known. Since the objective of the article is to evaluate the data belonging to the study area at first hand, it was avoided to give details of the method in the article (formulations and etc.). In the calculation of the IDW method the exponential p takes place. As the exponential values increases in IDW the effect becomes less in farther points. Although IDW has good results in terms of sampling points at frequent and equal weights, the results obtained may not always be accurate in the case of complex relationships with the environment studied. Also taking into account the fact that the sample collection points are frequent and equal, the p-exponent value was taken as 2. In this study, the principles and details of the method were not mentioned as it is not the part of this study. The element distribution maps were created using the ArcGIS 10.5 package program (Figure 4-14), which is a good method used for less than 1000 data.

The method of Kriging on the other hand has long been used synonymously with geostatistical interpolation. The fundamental of the method originates from the studies of mining engineer D.G. Krige and statistician H.S. Sichel (Krige, 1951). The technique has then become widespread thanks to the formulae derived by the French mathematician G. Matheron, and the method was named as the Kriging referring to D.G. Krige by G. Matheron (Cressie, 1993). In time, the technique has been further developed.

Kriging is an adjustable to many situations and flexible method considering many parameters. The Kriging can produce values for sampled points using the information beneath the spatial automatic correlation provided by semi-variograms in order to determine suitable weighting sets and to predict points and surfaces at non-sampled points. Since the semi-variogram is a function of distance, the weights vary according to the geographic arrangements of the samples. Low weights are assigned to distant patterns and high weights are assigned to nearby patterns. The Kriging also considers the relative positions of the samples with respect to each other. Ordinary Kriging is the most reliable method and can be used for many data sets. Although Simple Kriging forms more aesthetic contours it is less reliable. Using Universal Kriging is relatively difficult compared to others. As can be seen in figure 3, the majority of data belonging to the study area is skewed to the rightmost. As mentioned earlier, many transformation methods have been tried to normalize the data in order to transform it into normal distribution. The log transformation method among these methods yielded satisfactory results compared to the others in converting the given data. However, the data did not become an ideal normal distribution. Some of the data are skewed a little rightward while of some are skewed leftward. Therefore, the data to be used in the Kriging could not be transformed into an ideal normal distribution. However, the Kriging method was used considering that sampling points are frequent and regular. As mentioned above, although the common used method is the Ordinary Kriging method, the method was applied using Simple, Universal, and Log methods according to the characteristics of the data. Cross-validation is used is studying the accuracy of Kriging methods and in the performance assessment of the models used on Kriging surface. The cross-validation performed does not give a definitive answer on the validation of model whether it is correct or false. When the data show normal distributions, the Kriging gives good results. Otherwise, the transformations into normal distribution for data are made to use the method. Although data transformations contribute to elimination of skewness they may not always correct extreme roughness. However, in the study carried out by Chaplot et al. (2006) it was shown that although most of the interpolation techniques (natural neighborhood interpolation, spline interpolation and etc.) showed a similar performance when there is a frequent sampling, the IDW and Kriging methods gave better results where the number of points were not frequent and the distributions were irregular. In this study, sampling points are both frequent and regular. Nevertheless, the detailed evaluation, preliminary studies and cross-validation tests were conducted for the method of Kriging, but these studies were not included in the article because they are not part of the original purpose of the article and are preparatory studies. Given the fact that data obtained by the IDW method and maps produced by the Kriging method give closer results are taken into consideration, a cross validation of the method has been made in this way. The application summaries of the IDW and Kriging methods are given in Table 6. There are a lot of national and international studies both including the comparison of these methods and independent studies including IDW and Kriging methods (Akçay, 1998; Ağca, 2015; Patinha et al., 2008; Buttafuoco et al., 2010; Başaran et al., 2011; Zuo, 2011; Shuguang et al., 2015).

More detailed information on both techniques used in this article can be obtained especially in spatial statistics books (Cressie, 1990, 1993; Chiles and Delfiner, 1999; Ripley, 2004; Webster and Oliver, 2007; Hengl, 2009).

As it was aimed at presenting preliminary findings obtained in this study, the element distribution maps were produced by means of IDW and Kriging methods using the ArcGIS 10.5 package software in order to get first hand and fast information (Figure 4-14). Table

6 summarizes the operational processes of the subject methods.

Although there is not observed any strong correlation between the element concentrations obtained in the soil geochemistry study, there are some correlations between the elements in minor amounts. The single element distribution maps of the elements selected both in accordance with this correlation and the general geochemical principles were produced

Table 6- Process summary table of the Kriging and Inverse Distance Weighting Methods.

Kriging **Semi-variogram** **Considering neighboring points: Standard; Number of points considered: 5, at least 2 points were considered. Area type 4, 45°; Lag number: 12**	**Inverse Distance Weighting (IDW)** **Upper value: 2,** **Neighboring points studied: Standard,** **Neighboring point numbers studied:15 points, at least 10 points** **Field type: All**
Hg (69 samples) **Type:** Simple; **Output Type:** Predictive, **Conversion:** Normal Value Conversion; **Basic Distribution**: Gamma; **Main and Secondary semi axes:** 395,61; **Lag size:** 37,95; **Nugget:** 0.35; **Model Type:** Spherical; **Limit:** 395,1; **Partial threshold:** 0,82	**Hg (69 samples)** **Main and Secondary semi axes:** 543,71
Sb (142 samples) **Type:** Simple; **Output Type:** Prediction; **Conversion:** Normal Value Conversion; **Approach:** Density slope; **Basic distribution:** Log-normal; **Main and secondary axes:** 392,91; **Lag size:** 53,39; **Nugget :** 0,72; **Model Type:** Spherical; **Limit:** 392,9; **Partial threshold:** 0,37	**Sb (142 samples)** **Main and Secondary semi axes:** 575,71
As (287 samples) **Type:** Universal; **Output Type:** Predictive; **Orientation Type:** Stable; **Orientation Removal:** Local Polynomial Interpolation; **Upper value:** 0; **Main and secondary axes:**1834,87; **Lag size:** 212,88; **Nugget:** 854,09; **Model Type:** Spherical; **Limit:** 1834,86; **Partial threshold:** 202,87	**As (287 samples)** **Main and Secondary semi axes:** 648,99
Zn 285 (samples) **Type:** Universal; **Output Type:** Predictive; **Orientation Type:** Stable; **Orientation Removal:** Local Polynomial Interpolation; **Upper value:** 0; **Main and secondary axes:** 70,69; **Lag size:** 7,59; **Nugget:** 1786,69; **Model Type:** Spherical; **Limit:** 70,69; **Partial threshold:** 112,68	**Zn (285 samples)** **Main and Secondary semi axes:** 648,99
Pb (269 samples) **Type:** Universal; **Output Type:** Predictive; **Orientation Type:** Stable; **Orientation Removal:** Local Polynomial Interpolation; **Upper value:** 0; **Main and secondary axes:** 66,87; **Lag size:** 7.61; **Nugget:** 12319,26; **Model Type:** Stable; **Parameter:** 2; **Limit:** 66,87; **Partial threshold:** 3914,42	**Pb (269 samples)** **Main and Secondary semi axes:** 633,98
Mo (75 samples) **Type:** Simple; **Output Type:** Predictive; **Average:** 5,30; **Main and secondary axes:** 361,87; **Lag size:** 78,85; **Nugget:** 45,26; **Model Type:** Spherical; **Limit:** 361,87; **Partial threshold:** 11,48	**Mo (75 samples)** **Main and Secondary semi axes:** 556,43
Bi (40 samples) **Type:** Simple; **Output Type:** Predictive; **Orientation Type:** None; **Conversion:** Normal value conversion; **Approach:** Density slope; **Basic distribution:** Log-normal; **Main and secondary axes:** 1731,95; **Lag size:** 144,33; **Nugget:** 0,60; **Model Type:** Spherical; **Limit:** 1731,95; **Partial threshold:** 0,89	**Bi (40 samples)** **Main and Secondary semi axes:** 569,57
Cu (285 samples) **Type:** Simple; **Output Type:** Predictive; **Average:** 4,01; **Orientation Type:** None; **Conversion:** Log; **Main and secondary axes:** 483,89; **Lag size:** 46,25; **Nugget:** 0.50; **Model Type:** Spherical; **Limit:** 483,89; **Partial threshold:** 0,13	**Cu (285 samples)** **Main and Secondary semi axes:** 648,99
Ag (89 samples) **Type:** Simple; **Output Type:** Predictive; **Orientation Type:** None; **Conversion:** Normal value conversion; **Approach:** Density slope; **Basic distribution:** Log-normal; **Main and secondary axes:** 467,55; **Lag size:** 38,96; **Nugget:** 0,90; **Model Type:** Spherical; **Limit:** 467,55	**Ag (89 samples)** **Main and Secondary semi axes:** 647,66
Au (39 samples) **Type:** Simple; **Output Type:** Predictive; **Average:** 1,68; **Orientation Type:** None; **Conversion:** Log; **Main and secondary axes:** 936,24; **Lag size:** 119,14; **Nugget:** 0,16; **Model Type:** Spherical; **Limit:** 936,24; **Partial threshold:** 0,65	**Au (39 samples)** **Main and Secondary semi axes:** 546,.50
Sn (124 samples) **Type:** Simple; **Output Type:** Predictive; **Orientation Type:** None; **Conversion:** Normal value conversion; **Approach:** Density slope; **Basic distribution:** Log-empirical; **Main and secondary axes:** 563,15; **Lag size:** 49,38; **Nugget:** 0,59; **Model Type:** Spherical; **Limit:** 563,15; **Partial threshold:** 0,61	**Sn (124 samples)** **Main and Secondary semi axes:** 575,71

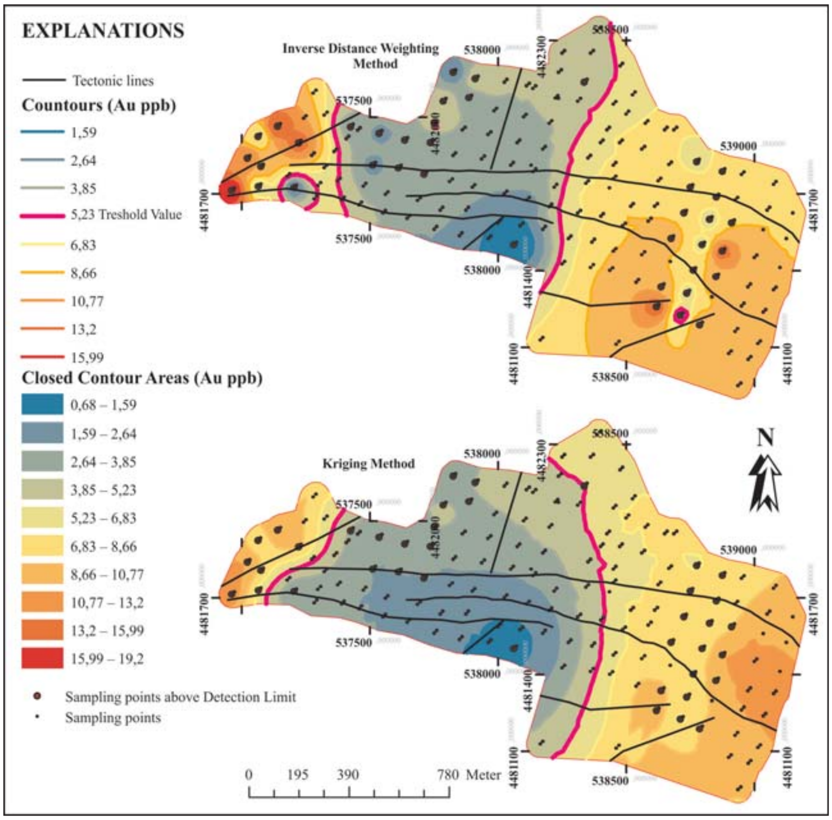

Figure 4- Distribution map generated by IDW and Kriging methods for Au element.

(Au, Ag, Cu, Pb, Zn, As, Sb, Bi, Mo, Sn and Hg) (Figures 4-14). For each element, the TV is obtained by adding M and 2MAD which are not affected much by end values as mentioned above. For each element, the element distribution maps, which had been drawn using IDW interpolation and Kriging methods, were shown together for easier interpretation.

Concentrations were found only in 39 sampling points for the gold element above the limit of detection and slightly above the mean shell values suggested by Rudnick and Gao (2010). It was seen that the TV of the gold concentrations for the area was above 5.23 µm/kg in W and in the E-SW directing sections where the argillic alteration had especially been developed (Figure 4). Although there was not detected any big difference between the map produced by the IDW interpolation and Kriging methods for Au distribution maps, it was seen that the sensitivity in the IDW method had been slightly higher (western and southeastern ends of the figure 4). The effect of tectonic elements in Au enrichment in the area is also observed on the map.

Ag element was detected above the detection limit at 89 sampling locations. It ranges between 0.02 and 28.95 mg/kg, and the calculated TV value for silver is 1.45 mg/kg (Figure 5). The silver values in the area occasionally exceed the upper crustal values suggested by Rudnick and Gao (2010). When element distribution maps generated by two different methods for silver element are examined, it is observed in the map generated by IDW method that Ag values are above TV (1.45 ppm) in the central part of the study area (Figure 5). Silver enrichments concentrates more heavily on areas where argillic and phyllic alterations develop. However, in the map generated by the Kriging method, the silver enrichment area is restricted into a smaller area. It would not be wrong to make an association with technological lines for silver element enrichments.

Cu element was detected above detection limits almost at all sampling points in the study area and TV for Cu was determined as 120 mg/kg by M + 2MAD method. When Cu element distribution maps were examined, there was not observed any remarkable Cu enrichment in the map produced by the Kriging method. Besides, Cu enrichments were noted especially in sections where phyllic alteration

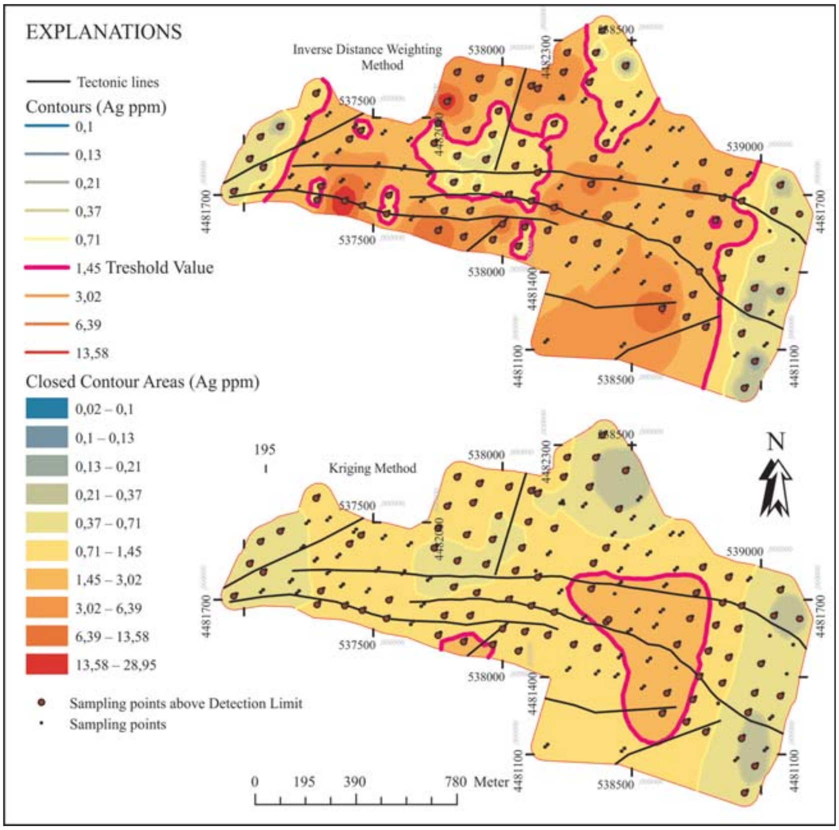

Figure 5- Distribution map generated by IDW and Kriging methods for Ag element

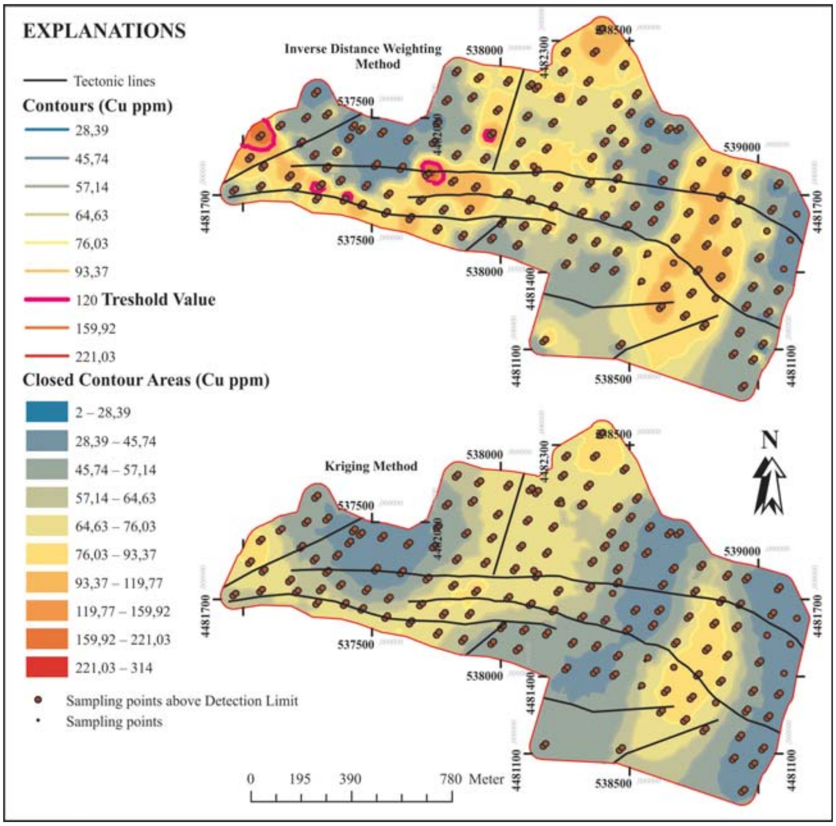

Figure 6- Distribution map generated by IDW and Kriging methods for Cu element.

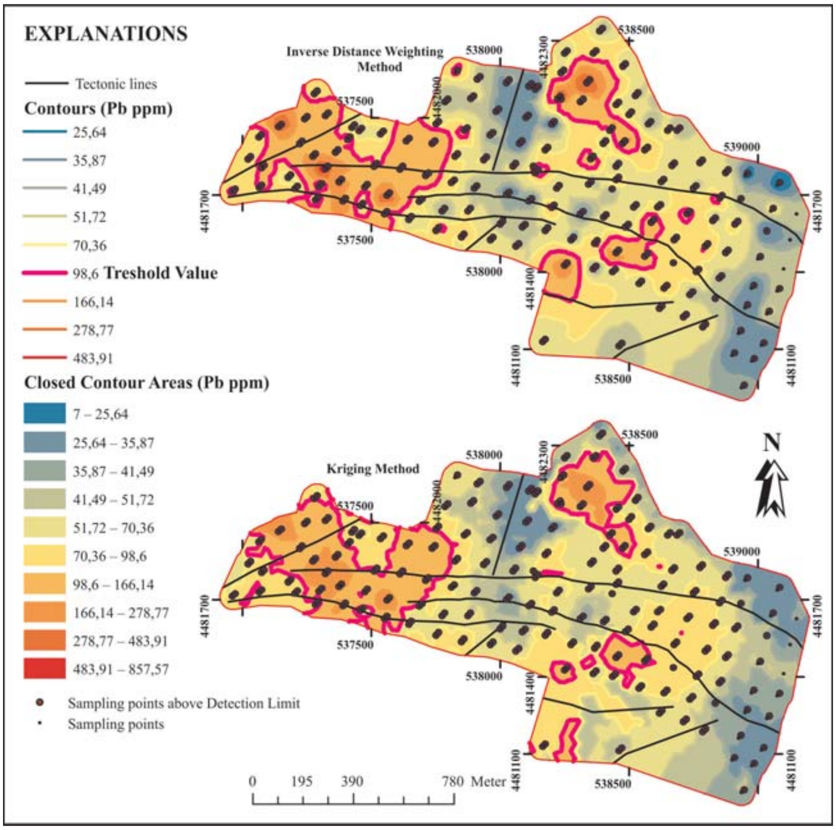

Figure 7- Distribution map generated by IDW and Kriging methods for Pb element.

had been observed, the western part of the study area (though in a limited area), in the map produced by IDW interpolation method (Figure 6). As Au element shows a correlation with Cu element though in weak amounts, this correlation should not be overlooked in detailed research studies that will be done in the field.

Pb element was detected at 269 sampling points above the detection limit in the study area. TV for lead was detected as 98.6 ppm by M+ 2MAD method and there are observed lead enrichments in west of the study area according to the element distribution maps (Figure 7) generated by IDW and Kriging methods. In the element distribution maps generated by both methods, the enriched areas coincide with each other.

Zn element was detected above the detection limit at 285 sampling points in the study area. The TV for Zn element was determined as 91 ppm by M + 2MAD method. Along with some differences in the Zn element distribution maps formed by IDW and Kriging methods, the areas of enrichment fall in the same zones, towards the central sections of the study area.

In the map generated by the IDW method, a small amount of enrichment is observed in a small area in the western part of the study area (Figure 8).

As element was determined above the detection limit at 287 sampling points in the study area. When the element distribution maps generated for the As element were examined, it was seen that As values were enriched in the western part, and these enrichments overlapped with the phyllic alteration areas (Figure 9). Although there was not observed any close relationship between Au and As elements in the correlation analysis, it was seen that the element distribution maps covered the As enrichment area coinciding with Au enrichment area. The fact that the correlation in the distribution map is not captured in the correlation analysis is due to the fact that the Au values are above the detection limit in the study area (Vural and Erdoğan, 2014).

Sb element in the Canca alteration area was found in concentrations above the detection limit at 142 sampling points. It shows a positive relationship with As element though not strong. There is observed Sb

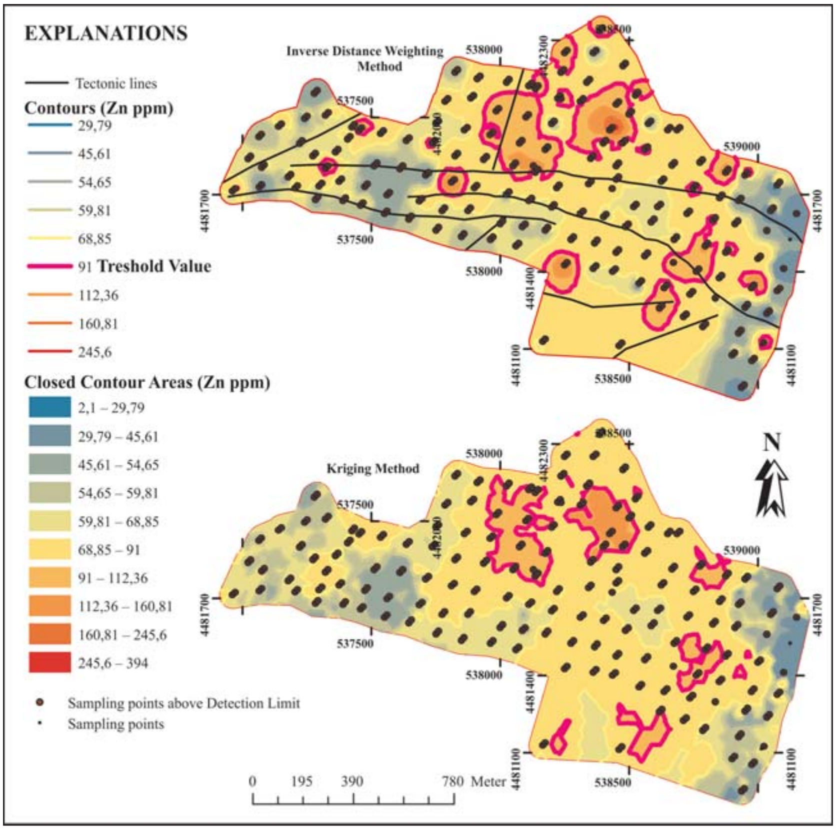

Figure 8- Distribution map generated by IDW and Kriging methods for Zn element.

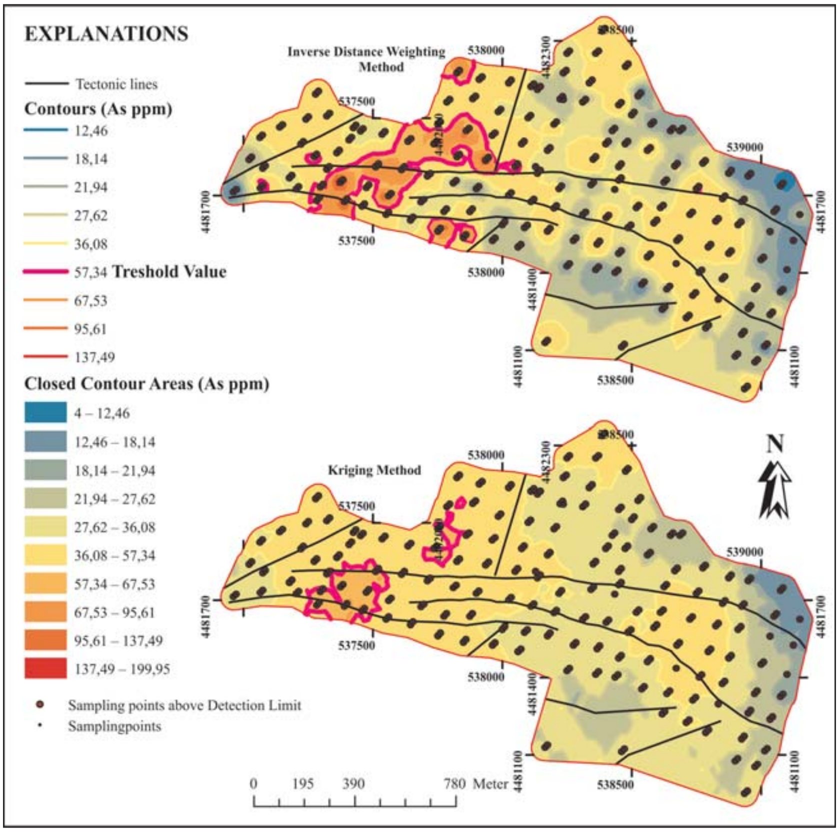

Figure 9- Distribution map generated by IDW and Kriging methods for As element.

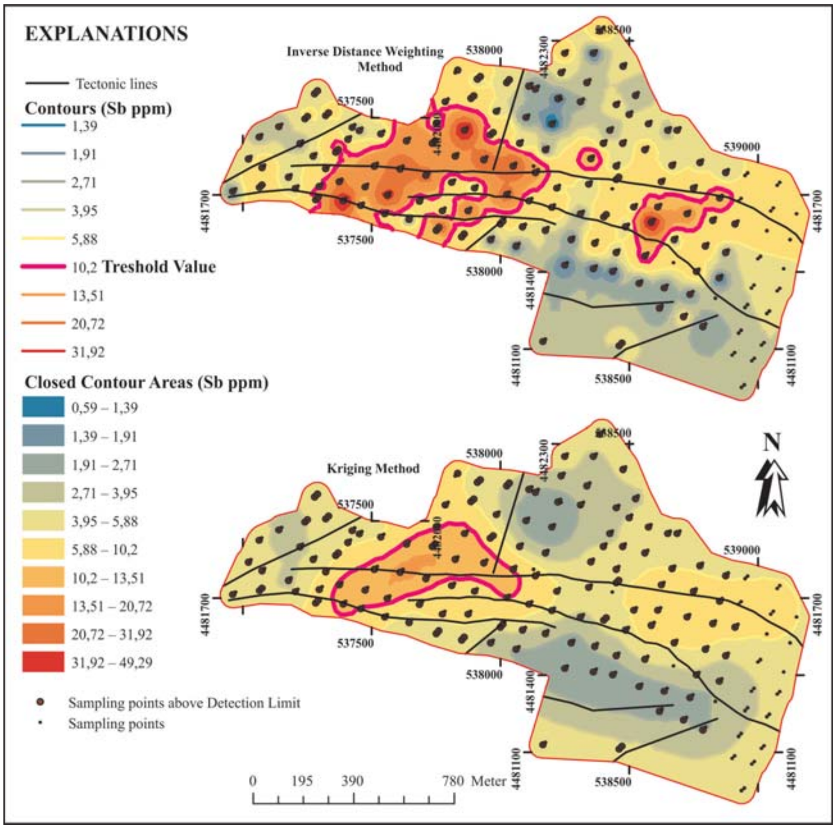

Figure 10- Distribution map generated by IDW and Kriging methods for Sb element.

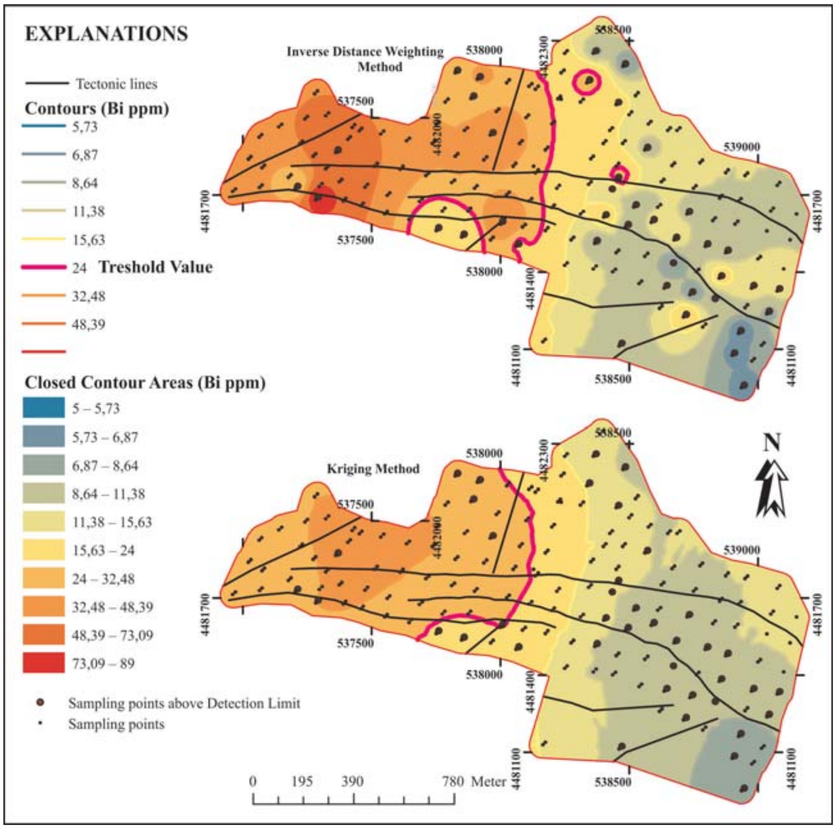

Figure 11- Distribution map generated by IDW and Kriging methods for Bi element.

enrichment in western part of the study area as a result of reflection of this relation in the element distribution maps prepared for Sb and in a limited area in the eastern part of the site in the distribution map generated by the IDW (Figure 10). The Sb enrichments have developed more in the phyllic alteration zone.

Bi element was detected above the detection limit at 40 sampling points and the enrichments in Sb were determined as it was in the western part of the study area (Figure 11). Tectonic lines become intense and get closer to each other in western part of the area and this shows that these tectonic activities are effective in element enrichment. It is seen that the element distribution map generated by the IDW method for Bi element gives more detail in the element distribution as well as in many elements.

Mo element has a concentration above the detection limit at 75 sampling points. In the calculation made by M + 2MAD method, the TV for Mo was found to be 6.77 ppm and it was seen that Mo enrichments in the study area were located in west of the study area where tectonic lines had become intense (Figure 12). Mo enrichments show close similarities with the enrichment areas of other elements. As in other elements, the element enrichment was more precisely detected in the element distribution map generated by the IDW method for Mo element (Figure 12).

Sn element was detected above the detection limit at 124 sampling points. When the element distribution maps prepared for Sn (IDW and Kriging Method) were examined, it was seen that tin enrichment was observed in the section where the argillic alteration occurred mainly in east of the study area (Figure 13). Minor enrichment is seen in the phyllic alteration zone to the west of the area.

Hg element occurred above the detection limit at only 69 sampling points. It was observed that Hg enrichments in the element distribution maps prepared by IDW and Kriging methods were in the eastern/central parts of the field. According to the distribution map generated by IDW method, some enrichments are also available in west of the study area (Figure 14). This element is seen to have spread to more detailed and wider areas looking at the element distribution map generated by the IDW method.

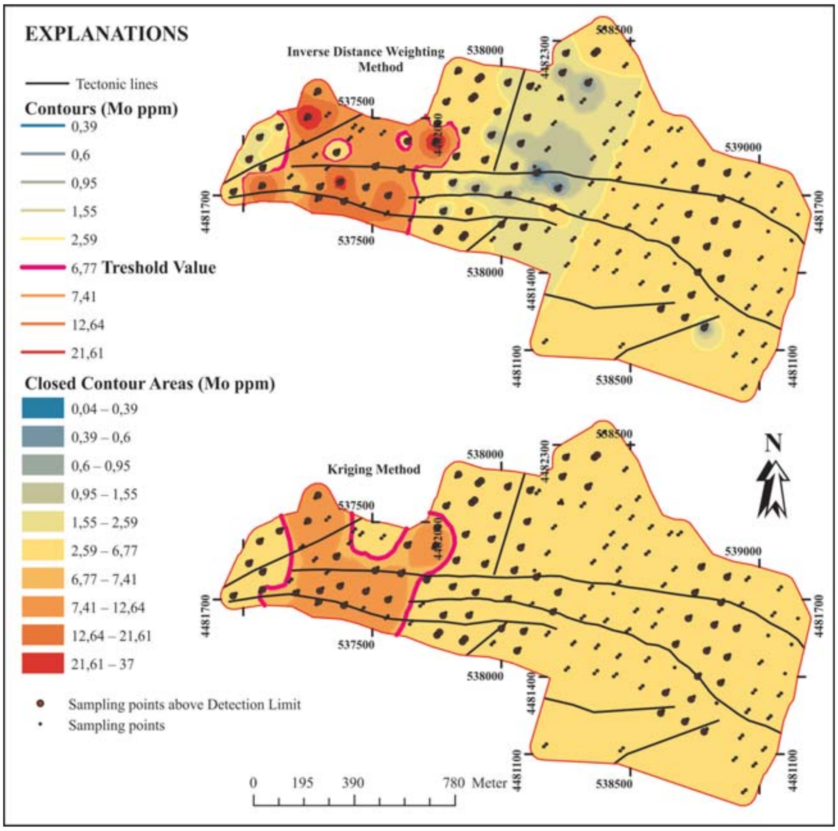

Figure 12- Distribution map generated by IDW and Kriging methods for Mo element.

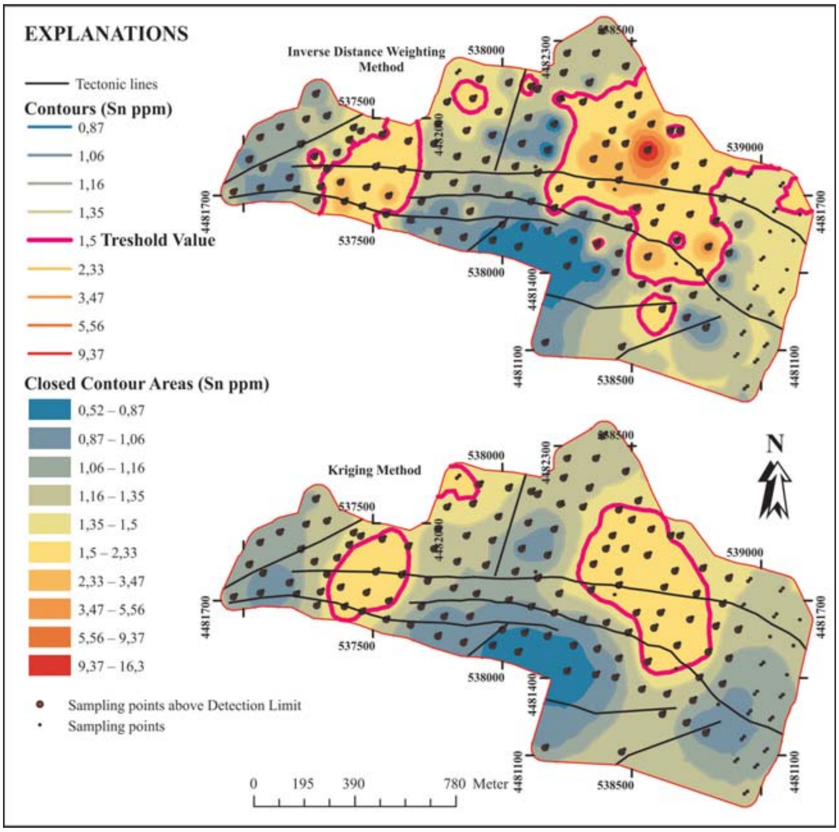

Figure 13- Distribution map generated by IDW and Kriging methods for Sn element.

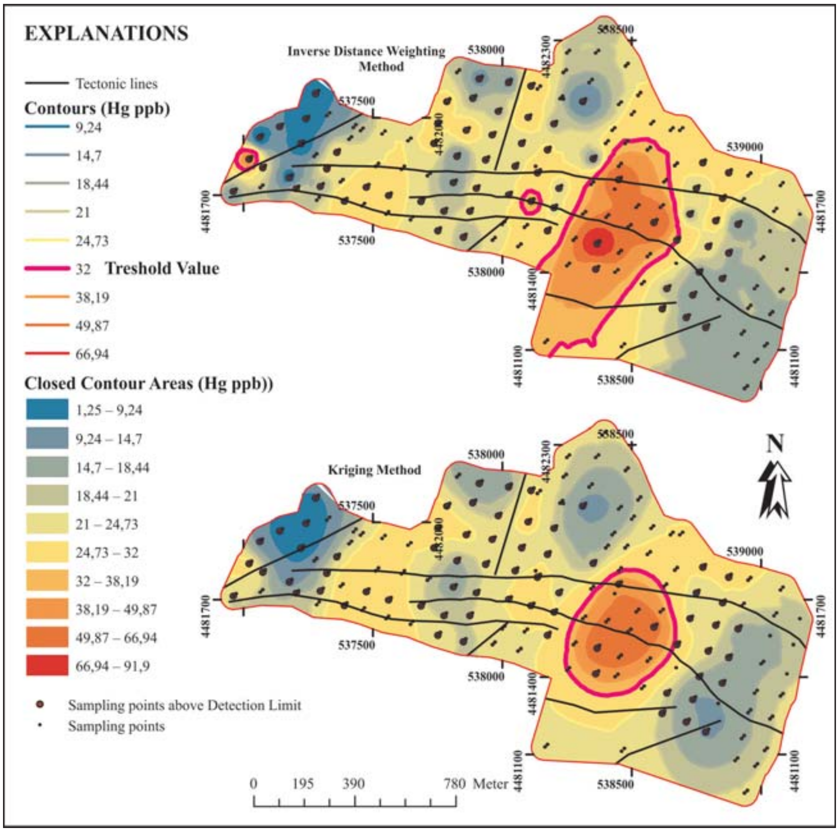

Figure 14- Distribution map generated by IDW and Kriging methods for Hg element.

4. Conclusions

In this study, the presence of soil geochemistry and possibly buried gold mineralization in the Canca (Gümüşhane) alteration area, where intensive alteration had been developed, were investigated. For this purpose, the total of 287 soil samples collected from the area were analyzed in terms of trace elements such as Cu, Pb, Zn, As, Sb, Bi, Mo, SN and Hg, which are pathfinder for gold and silver elements. The data obtained were evaluated by various statistical methods, threshold values belonging to the elements were determined by M+ 2MAD method and the distribution map of elements was generated by IDW and Kriging interpolation methods. IDW method is a well-known and widely used method ever since and it is also known that the later suggested Kriging method gives satisfactory results. These methods are also improved interpolation methods for estimating unknown points around any known sample point of interest (Matheron, 1971, 1963). When the element distribution maps generated by two mentioned methods were examined, it was seen that especially in the western part of the field, remarkable zoning/enrichment had been developed. The enrichment is predominantly in sections where tectonic lines become closer and the phyllic alteration develops, and this shows that alteration and tectonic activities are related to the enrichment. The Canca alteration area has been reported by MTA staffs in 1980s, and intensive alteration has been developed in the area. There have been carried out mapping studies at different scales at different times by MTA. Studies carried out on the area are mostly rock geochemistry studies. In the meantime, the exploratory drillings have been initiated in the area by the organization.

It is hoped that this and earlier geochemical studies carried out at different times in the Canca area will make an important contribution to drilling works currently being carried out by MTA. Therefore, it is suggested to make plan considering the element enrichment and zonations which are detected by the soil geochemistry in exploration and drilling works to be carried out in the area. When the area is investigated in detail, the presence of landslides developed in the eastern part at low altitudes should be considered in plans to be made and the element enrichment/anomaly areas observed in this section should be considered cautiously.

When IDW and Kriging methods used to generate the element distribution maps and data sets for the area were compared, it was seen that the element distribution maps made by the IDW interpolation method gave better results. In other words, the anomaly contrast resolution is higher in the element distribution maps generated by the IDW interpolation method. When all these data obtained in the soil geochemistry study are evaluated together, it was concluded that the detailed drilling and geophysical studies to be carried out for gold mineralization on the area had importance and it would be more appropriate to perform these studies in the western part of the study area.

Acknowledgements

This study was supported by the TUBITAK Project number 113Y569. Some analyzes were repeated in laboratories of the General Directorate of Mineral Research and Exploration for comparison. The author would like to thank to the MTA General Directorate and its employees for their contributions to the analysis. The author also thanks to Mr. Sebahattin Güner (Retired MTA General Directorate Personel) for sharing their experience of almost 30 years in the field of Canca and to trainee students Şükrü Bulut, Mert Karaaslan and Emre Topçu for their assistance on the field and in the laboratory work.

References

Ağca, N. 2015. Spatial distribution of heavy metal content in soils around an industrial area in Southern Turkey. Arab J Geosci. 8(2):1111-1123.

Akçay, M. 1998. Lâdik-Sızma (Konya) civa yatakları çevresinde element dağılım profilleri ve altın-gümüş ve baz metal potansiyeli: Jeokimyasal ve istatistiksel bir yaklaşım. Türkiye Jeoloji Bülteni, 41(1):37-47.

Almasi, A., Jararirad, A., Afzal, P., Rahimi, M. 2015. Orogenic Gold Prospectivity Mapping Using Geospatial Data Integration, Region of Saqez, NW Of Iran (Jeospatial Veri Entegrasyonu ile Orojenik Altın Prospeksiyon Haritasının Oluşturulması, Saqez Bölgesi, Kb İran). Bull. Miner. Res. Explor. 150, 67–78.

Anderson, D.A.J.S. 2008. Quantitative Analysis of Tin- and Tungsten-Bearing Sheeted Vein Systems. Economic Geology, 103 (5): 1043-1056.

Arslan, M., Aliyazıcıoğlu, I. 2001. Geochemical and petrological characteristics of the Kale (Gümüşhane) volcanic rocks: Implications for the Eocene evolution of eastern Pontide arc volcanism, northeast Turkey. Int. Geol. Rev. 43, 595–610. doi:10.1080/00206810109465035

Başaran, M., Erpul, G., Özcan, A.U., Saygın, D.S., Kibar, M., Bayramın, I., Yılman, F.E. 2011. Spatial information of soil hydraulic conductivity and performance of cokriging over kriging in a semi-arid basin scale. Environ Earth Sci, 63:827–838. Doi: 10.1007/s12665-010-0753-6.

Buttafuoco, G., Tallarico, A., Falcone, G., Guagliardi, I. 2010. A geostatistical approach for mapping and uncertainty assessment of geogenic radon gas in soil in an area of southern Italy. Environ Earth Sci, 61:491–505. Doi: 10.1007/s12665-009-0360-6.

Carranza, E.J.M. 2009. Controls on mineral deposit occurrence inferred from analysis of their spatial pattern and spatial association with geological features. Ore Geol. Rev. 35, 383–400. doi:10.1016/j.oregeorev.2009.01.001

Carranza, E.J.M., Sadeghi, M. 2010. Predictive mapping of prospectivity and quantitative estimation of undiscovered VMS deposits in Skellefte district (Sweden). Ore Geol. Rev. 38, 219–241. doi:10.1016/j.oregeorev.2010.02.003

Carranza, E.J.M., Owusu, E.A., Hale, M. 2009. Mapping of prospectivity and estimation of number of undiscovered prospects for lode gold, southwestern Ashanti Belt, Ghana. Miner. Depos. 44, 915–938. doi:10.1007/s00126-009-0250-6

Chaplot, V., Darboux, F., Bourennane, H., Leguedois, S., Silvera, N., Phachomphon, K. 2006. Accuracy of interpolation techniques for the derivation of digital elevation models in relation to landform types and data density. Geomorphology 77, 126–141.

Cheng, Q. 2008. Modeling local scaling properties for multiscale mapping. Vadose Zone Journal 7, 525–532.

Chiles, J. P., Delfiner, P. 1999. Geostatistics: modeling spatial uncertainty. John Wiley and Sons, New York, s. 720.

Cressie, N. A. C. 1990. The origins of kriging. Mathematical Geology 22 (3): 239–252.

Cressie, N.A.C. 1993. Statistics for Spatial Data, revised ed. ed. John Wiley and Sons, New York.

Çınar, S., Türk, O., Er, M., Güç, A.R., Musaoğlu, A., Gümüşel, A., Özdemir, M., Kurtoğulu, T. 1982. Gümüşhane İli ve Güneybatısının Jeolojisi Raporu. Maden Tetkik ve Arama Genel Müdürlüğü Rapor No: 7696, Ankara-Türkiye (unpublished).

Dokuz, A. 2011. A slab detachment and delamination model for the generation of Carboniferous high-potassium I-type magmatism in the Eastern Pontides, NE Turkey: The Köse composite pluton. Gondwana Res. 19, 926–944. doi:10.1016/j.gr.2010.09.006

Eyüboğlu, Y., Santosh, M., Dudas, F.O., Chung, S.L., Akaryalı, E. 2011. Migrating magmatism in a continental arc: Geodynamics of the Eastern Mediterranean revisited. J. Geodyn. 52, 2–15. doi:10.1016/j.jog.2010.11.006

Güner, S., Er, M., Gümüşel, A., Boğuşlu, M. 1985. Gümüşhane-Eski Gümüşhane yöresindeki cevherleşmelere ait jeoloji raporu. Rapor No: 8029. General Directorate of Mineral Research and Exploration, Ankara-Turkey (unpublished).

Güner, S., Yazıcı, E.N. 2008. Gümüşhane Bayburt Yörelerine Ait Epitermal Altın Aramaları Raporu. Rapor No: 11075. General Directorate of Mineral Research and Exploration, Ankara-Turkey (unpublished).

Güven, İ. 1993. Doğu Pontidlerin 1/25000 Ölçekli Kompilasyonu. General Directorate of Mineral Research and Exploration, Ankara-Turkey.

Hampel, F.R. 1974. The influence curve and its role in robust estimation. J. Am. Stat. Assoc. 69, 383–393.

Hengl, T. 2009. A practical Guide to Geostastical Mapping. 2nd editon. Office for Official Publications of the European Communities, Luxembourg (ISBN: 978-92-79-06904-8).

Jena, D.O. 1996. Interesting Papers in Other Journals. Geology 91, 228–237.

Kandemir, R. 2004. Gümüşhane ve Yakın Yörelerindeki Erken-Orta Jura Yaşlı Şenköy formasyonunun Çökel Özellikleri ve Birikim Koşulları. Trabzon.

Kansız, H., Akıncı, S., Kurtoğulu, T., Türkmen, S., Yılmaz, Z., Ağan, A. 1994. Doğu Pontid Güney Zonu Epitermal Altın Aramaları. General Directorate of Mineral Research and Exploration, Ankara-Turkey.

Karslı, O., Uysal, I., Dilek, Y., Aydın, F., Kandemir, R. 2013. Geochemical modelling of early Eocene adakitic magmatism in the Eastern Pontides, NE Anatolia: continental crust or subducted oceanic slab origin? Int. Geol. Rev. 55, 2083–2095. doi:Doi 10.1080/01431161.2013.819958

Kaygusuz, A., Siebel, W., Şen, C., Satır, M. 2008. Petrochemistry and petrology of I-type granitoids in an arc setting: The composite Torul pluton, Eastern Pontides, NE Turkey. Int. J. Earth Sci. 97, 739–764. doi:10.1007/s00531-007-0188-9

Ketin, I. 1966. Tectonic units of Anatolia (Asia Minor). Maden Tetkik ve Arama Genel Müdürlüğü Dergisi 66, 23–34.

Krige, D.G. 1951. A statistical approach to some basic mine valudation problems on the Witwatersrand. J. Chem. Metall. Min. Soc. 52, 119–139.

Matheron, G. 1963. Principals of geostatistics. Economic. Econ. Geol. 58, 1246–1266.

Matheron, G. 1971. The theory of regionalized variables and its application. Cent. Morphol. Math. Fontainebleau, Cah. 5, 211.

MTA, 1986. The Republic of Turkey report on the cooperative mineral exploration of Gümüşhane area, consolidated report. General Directorate of Mineral Research and Exploration, Ankara-Turkey.

Patinha, C., Correia, E., Ferreira da Silva, E., Simões, A., Reis, P., Morgado, F., Cardoso Fonseca, E. 2008. Definition of geochemical patterns on the soil of Paul de Arzila using correspondence analysis. Journal of Geochemical Exploration 98: 34–42.

Pelin, S. 1977. Alucra (Giresun) Güneydoğu yöresinin petrol olanaklan bakımından jeolojik incelemesi. Karadeniz Teknik Üniversitesi Yayını, Yayın No. 87, Trabzon.

Reiman, C., Filzmoser, P. 2000. Normal and lognormal data distribution in geochemistry: death of a myth. Consequences for the statistical treatment of geochemical and environmental data. Environ. Geol. 39, 1001–1014.

Reis, A.P., Sousa, A.J., Cardoso Fonseca, E. 2001. Soil geochemical prospecting for gold at Marrancos (Northern Portugal). J. Geochemical Explor. doi:10.1016/S0375-6742(01)00169-8

Ripley, B. D. 2004. Spatial statistics, 4th Edition. Wiley-IEEE, London, s. 252.

Rose, A.W., Hawkes, H., Webs, J. 1991. Geochemistry in Mineral Exploration, 2nd ed. Academic Press, Londan, England.

Rudnick, R., Gao, S. 2010. Composition of the Continental Crust, in: Holland, H., Turekian, K. (Eds.), Readings of Treatise on Geochemistry. Elsevier, Londan, England.

Shepard, D. 1968. A two-dimensional interpolation function for 52 irregularly-spaced data, in: Blue, R.B.S., Rosenberg, A.M. (Eds.), Proceedings of the 1968 ACM National Conference. ACM 54 Press, New York, pp. 517–524.

Shuguang, Z., Kefa, Z., Yao, C., Jinlin, W., Jianli, D. 2015. Exploratory data analysis and singularity mapping in geochemical anomaly identification in Karamay, Xinjiang, China. Journal of Geochemical Exploration 154:171–179. doi.org/10.1016/j.gexplo.2014.12.007.

Tobler, W. R. 1970. A computer model simulation of urban growth in the detroit region. Economic Geography 46 (2): 234–240.

Tokel, S. 1972. Stratigraphical and volcanic history of Gümüşhane region.

Topuz, G., Altherr, R., Schwarz, W.H., Dokuz, A., Meyer, H.P. 2007. Variscan amphibolite-facies rocks from the Kurtoğlu metamorphic complex (Gümüşhane area, Eastern Pontides, Turkey). Int. J. Earth Sci. 96, 861–873. doi:10.1007/s00531-006-0138-y

Tume, P., Bech, J., Reverter, F., Bech, J., Longan, L., Tume, L., Sepulveda, B. 2011. Concentration and distribution of twelve metals in Central Catalonia surface soils. J. Geochemical Explor. 109, 92–103. doi:10.1016/j.gexplo.2010.10.013.

Vural, A. 2006. Bayramiç (Çanakkale) ve Çevresindeki Altın Zenginleşmelerinin Araştırılması. Ankara Üniversitesi, Ankara Türkiye.

Vural, A. 2014. Trace/heavy metal accumulation in soil and in the shoots of acacia tree, Gümüşhane-Turkey. Bulletin of the Mineral Research and Exploration, 148, 85–106.

Vural, A. 2017. K-Ar Dating for Determining the Age of Mineralization as Alteration Product : A Case Study of Antimony Mineralization Vein Type in Granitic Rocks of Gümüşhane Area , Turkey 132, 792–795. doi:10.12693/APhysPolA.132.792

Vural, A., Erdoğan, M. 2014. Eski Gümüşhane Kırkpavli Alterasyon Sahasında Toprak Jeokimyası. Gümüşhane Üniversitesi Fen Bilim. Enstitüsü Derg. 4, 1–15.

Webster, R., Oliver, M.A. 2007. Geostatistics for Environmental Scientist. 2nd editon, John Wiley and Sons, Ltd. İngiltere. s. 315

Yaylalı-Abanuz, G., Tüysüz, N., Akaryalı, E. 2012. Soil geochemical prospection for gold deposit in the Arzular area (NE Turkey). J. Geochemical Explor. 112, 107–117. doi:10.1016/j.gexplo.2011.08.004

Yazıcı, E.N., Dursun, Ö., Güner, S. 2014. Gümüşhane-Bayburt-Artvin Epitermal Altın Aramaları Raporu. General Directorate of Mineral Research and Exploration, Ankara-Turkey.

Yılmaz, Y. 1972. Petrology ancj structure of the Gümüşhane granite and surrounding rocks, NE Anatolia.

Zuo, R. 2011. Identifying geochemical anomalies associated with Cu and Pb–Zn skarn mineralization using principal component analysis and spectrum–area fractal modeling in the Gangdese Belt, Tibet (China J. Geochemical Explor. 111:13–22.

Zuo, R., Cheng, Q., Agterberg, F.P., Xia, Q. 2009. Evaluation of the uncertainty in estimation of metal resources of skarn tin in Southern China. Ore Geol. Rev. 35, 415–422. doi:10.1016/j.oregeorev.2008.12.001.